PHYSICAL REVIEW B, VOLUME 64, 060101(R)

# Long-ranged ferroelectric interactions in perovskite superlattices

M. Sepliarsky,[1,2] S. R. Phillpot,[1] D. Wolf,[1] M. G. Stachiotti,[2] and R. L. Migoni[2]
[1]*Materials Science Division, Argonne National Laboratory, Argonne, Illinois 60439*
[2]*IFIR, Universidad Nacional de Rosario–CONICET, Rosario, Argentina*
(Received 1 May 2001; published 3 July 2001)

Atomistic simulations show that there are long-ranged ferroelectric interactions between the ferroelectric layers in ferroelectric/paraelectric superlattices mediated by continuous chains of polarization running through the intervening paraelectric layers. The resulting behavior of the superlattice is strongly dependent on the modulation length. At short modulation lengths the superlattice acts as a single-component system; at long modulation lengths the individual ferroelectric layers act almost independently.

DOI: 10.1103/PhysRevB.64.060101 PACS number(s): 77.80.Bh, 77.84.Dy

Current interest in superlattices containing ferroelectric materials is driven by the vision of building nanostructures with ferroelectric, dielectric, and optical properties unachievable in either the bulk or in solid solutions. Such nanostructures can be expected to have important applications in, e.g., ferroelectric memories, sensors, microelectromechanical systems, and optical devices. Among the heterostructures grown have been ferroelectric/paraelectric superlattices [including $BaTiO_3/SrTiO_3$ (Refs. 1–3), $KNbO_3/KTaO_3$ (Refs. 4–6), and $PTiO_3/SrTiO_3$ (Ref. 7)] and ferroelectric/ferroelectric superlattices [$PbTiO_3/BaTiO_3$ (Ref. 8)]. While there is experimental evidence for a strong dependence of the properties of such superlattices on modulation length, the underlying physics controlling their properties is only poorly understood.

In this Rapid Communication we elucidate the role of the modulation length, substrate strain, and the interfaces on the properties of a perovskite superlattice. We focus on a $KNbO_3/KTaO_3$(KNO/KTO) superlattice because it is representative of the most widely studied ferroelectric/paraelectric class of heterostructures, and because the absence of any intrinsic polarization in the paraelectric layer makes the interface-induced effects particularly easy to identify. Using atomic-level computer simulations, we show that (i) while the in-plane components of polarization are only weakly coupled across the interfaces, the components of polarization along the modulation direction are strongly coupled, (ii) the ferroelectric layers interact via the induced polarization in the intervening paraelectric layers, and (iii) when the modulation wavelength is sufficiently short this interaction leads the superlattice to behave as a single artificial ferroelectric material. Together, these insights provide an essential first step towards a systematic understanding of the intrinsic properties of ferroelectric/paraelectric heterostructures.

Atomic-level simulations with the shell-model potentials for KNO and KTO used in this study have described well the phase behavior and properties of KNO and KTO perfect crystals.[9] In particular, we found that KNO is ferroelectric at $T=0$ K with a simulated lattice parameter of 4.034 Å and a rhombohedral angle of 89.3° and that KTO is paraelectric at all temperatures with a simulated zero-temperature lattice parameter of 4.005 Å.[9] Moreover, when used in combination, the potentials reproduced the ferroelectric properties of $KTa_{0.5}Nb_{0.5}O_3$ (KTN) random solid solutions.[9]

Using these potentials, we have simulated the zero-temperature structure and properties of coherent (001) KNO/KTO superlattices of equal layer thicknesses and various modulation lengths $\Lambda$ (i.e., the total thickness of a KNO/KTO bilayer, measured in unit cells); each interface lies at a KO plane shared by neighboring layers and thus all interfaces are crystallographically identical to each other. Their structures and switching properties of these superlattices have been determined with standard atomistic-simulation techniques. In particular, periodic border conditions are applied to the simulation cell in all three spatial directions; thus the simulation cell may be envisaged as a part of a KNO/KTO superlattice far away from both the substrate and the free surface neither of which is explicitly simulated. All the ions were initially placed at positions corresponding to the perfect crystal at zero temperature. The equilibrated zero-temperature structure was then determined by a zero-temperature quench until the force on each individual core and shell was less than 0.05 eV $Å^{-1}$. Since the simulations were intended to model a superlattice on a KTO substrate, the in-plane lattice parameter was fixed to that of KTO at zero temperature; however since the heterostructure is not under any constraint in the modulation direction, the length of the simulation cell in the $z$ direction was allowed to expand or contract to reach zero stress. The polarization was determined from the core-shell displacements and the displacements of the ions from their centrosymmetric positions. The external electric field $E_z$ was imposed via an additional force $F_z=qE_z$ on each core and shell of charge $q$.

To obtain a fully equilibrated structure, it is important that the interior regions of each layer be capable of assuming the symmetry of the corresponding perfect crystal; therefore, as shown in the sketch at the top of Fig. 1, we simulate four layers in the superlattice with the two rhombohedral KNO layers initially being polarized in the [111] and $[\bar{1}\bar{1}1]$ directions.

Figure 1 shows the variation in the polarization in the modulation direction $P_z$ (solid circles) and in the $x$-$y$ plane, $P_x=P_y$ (open circles) averaged over unit-cell-thick slices through the $\Lambda=36$ superlattice. In analyzing these polarization profiles, we first address the strain effects produced by the KTO substrate, which result in a compressive strain of $\sim$0.7% on the KNO layers. To compensate for this in-plane compression, the KNO layers expand in the $z$ direction

 

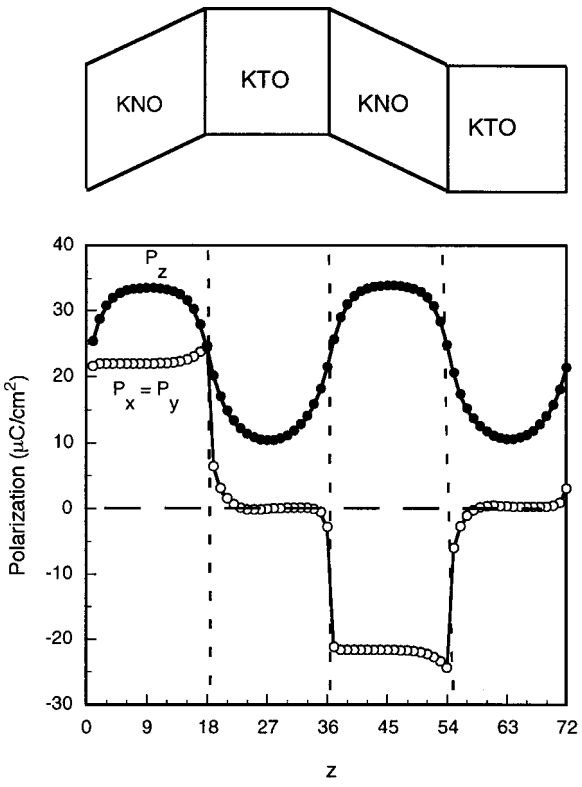


FIG. 1. Schematic of the simulated KNO/KTO superlattice (top) and spatial dependence of the polarization in the plane $P_x = P_y$ (open circles) and in the modulation direction $P_z$ (solid circles) for a superlattice with $\Lambda = 36$ and in-plane lattice parameters corresponding to a KTO substrate.

thereby breaking the strict rhombohedral symmetry of the polarization of KNO; nevertheless, these strains are not sufficient to force the KNO to become tetragonally polarized. Moreover, the magnitudes of the polarization in the interiors of the KNO layers ($|P_x| = 21.7\,\mu\text{C/cm}^2$, $P_z = 33.4\,\mu\text{C/cm}^2$) are the same as those calculated independently for a perfect crystal under the same strain conditions; the opposite signs of $P_x$ in the two layers arise from the equal and opposite rhombohedral distortions of the KNO layers. Similarly, the absence of any in-plane polarization for the KTO layer is consistent with the absence of any strain arising from the KTO substrate. The finite value of $P_z$ in the interior of the KTO layer, however, is different from the expected value of $P_z = 0$ for this unstrained layer, which, as we discuss below, has important consequences for the ferroelectric properties of the heterostructure.

The components of polarization in the $x$-$y$ plane and in the modulation direction show remarkably different behaviors at the interfaces. The rather abrupt transitions in $P_x$ at the interfaces are indicative of only rather weak coupling between the in-plane components of the polarization along the modulation direction. In addition, the presence of a weak coupling between $P_x$ and $P_z$ results in $P_x$ in the interface regions being slightly different in the cases of $P_z$ is pointing into and out of the ferroelectric layer (see Fig. 1).

By contrast with $P_x$, $P_z$ varies continuously through the interfaces, a signature of strong coupling. The penetration length, determined from the approximately exponential change in $P_z$ in the interface region, is only about two lattice parameters in the KNO layer for all values of $\Lambda$ simulated, but appears to increase with increasing $\Lambda$ for the KTO layer. Therefore, to characterize the penetration of the polarization into the KTO layer, we define the values of $P_z$ and of the $z$ component of the lattice strain at the center of the KTO layers as $P_c$ and $s_c$, respectively. We expect that for thick enough KTO layers (i.e., above some critical value of the modulation wavelength $\Lambda_\infty$), $P_c$ and $s_c$ will converge to their perfect-crystal values of $P_c = 0$ and $s_c = 0$. To estimate $\Lambda_\infty$, we analyze the finite-size effects by plotting $P_c$ and $s_c$ as a function of $1/\Lambda$ in Fig. 2. While it is evident from the absence of a linear regime that we cannot estimate $\Lambda_\infty$ from $P_c$ (solid squares), a fit to $s_c$ (open squares), which does display linear behavior in the low-$1/\Lambda$ regime (dotted line), yields an extrapolated estimate of $\Lambda_\infty \sim 160$ ($\sim$640 Å). Thus the strain in the interior of a KTO layer only vanishes for layers of more than 80 unit cells thick. While, strictly speaking, this is a measure of the penetration length of the structural changes into the KTO layer, given the nonlinearity in the dependence of $P_c$, it may also be taken as a lower-bound estimate for the penetration length of the polarization into the KTO layer. The marked difference between the penetration lengths in the layers is consistent with the large difference in the dielectric constants $\varepsilon$ of the two materials, which measure the ease with which they can be polarized: while $\varepsilon$(KNO) is $\sim$50, $\varepsilon$(KTO) is $\sim$3000. Despite this long-ranged penetration of $P_z$ into the KTO layers, we find that the values of $P_z$ at the interfaces themselves are remarkably independent of $\Lambda$ and take a value very similar to that of a KTN solid solution under these strain conditions.

The above analyses have clearly demonstrated the importance of interface effects on the properties of the superlattices. To elucidate how these effects are coupled to the strain we have also simulated superlattices under strain conditions corresponding to a KNO substrate at $T = 0$ K. As in the case of the KTO substrate, both components of polarization in the KNO layers and the in-plane polarization in the KTO layers rapidly reach the values corresponding to these strain conditions. In particular, the KTO layer becomes ferroelectric with an in-plane polarization along the [110] direction; however, there remains a small component of polarization in the $z$ direction in the KTO that cannot be explained by strain. As for the case of the KTO substrate, $P_x$ changes abruptly through the interfaces while $P_z$ varies continuously through the interfaces; its value at the interface also being the same as the solid solution under these strain conditions. Based on this analysis we conclude, therefore, that the strain effects and the interface effects are essentially decoupled. The general validity of this conclusion for ferroelectric/paraelectric superlattices is indicated by the rather similar results we have obtained for $BaTiO_3/SrTiO_3$ superlattices.

A consistent framework in which to understand these effects comes from a consideration of the anisotropy in the correlation of the polarization dipoles in ferroelectrics. This, so-called, Lorentz field[10] arises from the significant mutual enhancement of the dipole moments of Nb (and Ta) ions and

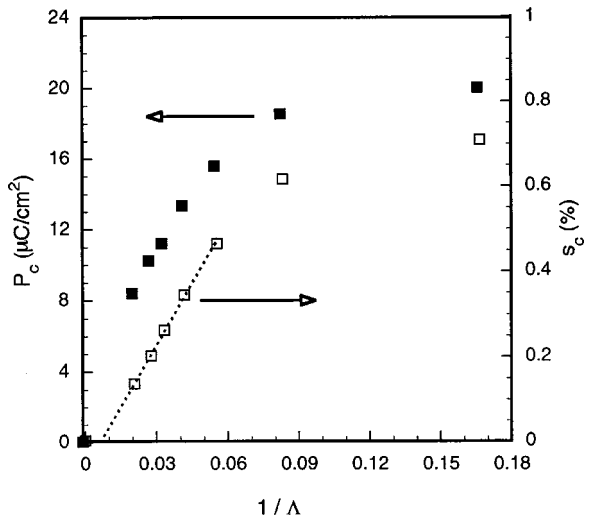


FIG. 2. The dependence of the $z$ component of polarization and $z$ component of lattice strain at the center of the KTO layer, $P_c$ and $s_c$ (solid and open squares, respectively), on the inverse modulation length $1/\Lambda$. The linear region of the strain curve (dotted line) extrapolates to zero strain at $\Lambda_\infty \sim 160$.

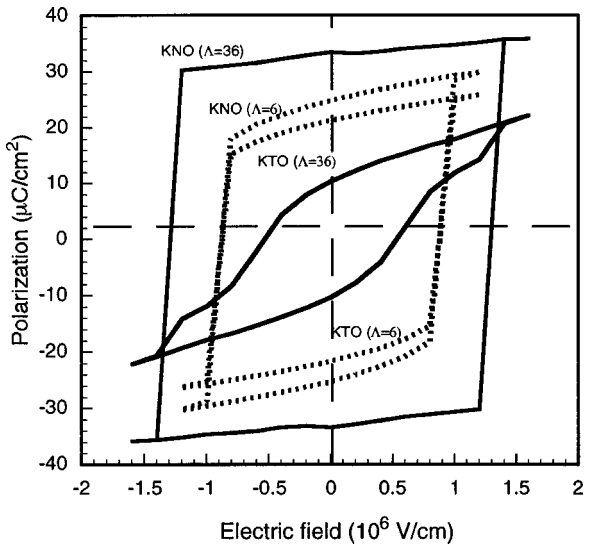


FIG. 3. Hysteresis loops for the KNO and KTO layers in superlattices with $\Lambda = 36$ (solid lines) and the $\Lambda = 6$ (dotted lines). While the KTO layer for $\Lambda = 36$ appears to be ferroelectric, physically, however, it behaves as a paraelectric under the combined external field and the electric field produced by the KNO layers.

O ions lying along the direction of polarization. By contrast, in the direction normal to the polarization, there is only a very weak interaction between the dipoles of the Nb (Ta) ions and the O ions. As a consequence, strongly correlated chains of polarization tend to form, with only rather weak correlations in the direction normal to the chains. This anisotropy in the Lorentz field is manifested in these superlattices as the long-ranged correlations in $P_z$ across the interfaces and only very short-ranged correlations in $P_x$.

These results naturally raise the question as to whether these superlattices can be considered as behaving a distinct, though coupled, layers or rather as a single composite material. Indeed, experiments on KNO/KTO superlattices show that for long modulation wavelengths the KNO layers are almost independent of each other. By contrast, for $\Lambda < 12$ the Curie temperature is essentially $\Lambda$ independent with a value corresponding to the KTN solid solution;[5] i.e., the superlattices behave as a single artificial ferroelectric material. It was suggested that this behavior arises from ''long-ranged ferroelectric interactions,'' the exact nature of which was not clearly defined.[5] As we now show, these long-ranged ferroelectric interactions arise from the coupling of the ferroelectric layers through the polarization induced in the intervening paraelectric layers. There is an analogous effect in ferromagnetic heterostructures,[11] albeit mediated by exchange interactions rather than induced polarization.

To elucidate the nature of the long-ranged ferroelectric interactions, we have simulated the ferroelectric switching of superlattices of varying modulation lengths. Figure 3 shows calculated hysteresis curves for unit-cell-thick slices at the center of the KNO and KTO layers for the representative cases of $\Lambda = 6$ and 36. For $\Lambda = 6$, the loops for KNO and KTO are almost identical, indicating that the superlattice does, indeed, act as a single artificial ferroelectric structure with the response of the KTO layers being controlled by the ferroelectric KNO layers. For $\Lambda = 36$, the KNO layers show a square hysteresis loop characteristic of a good ferroelectric. The KTO layers also appear to show a ferroelectric hysteresis loop; however, this is simply an effect of coupling to the KNO layers. In particular, no hysteretic behavior appears in the KTO layers under a cyclic electric field applied only to one of them when the KNO layers are not allowed to switch. Thus, the KTO layers actually behave as a paraelectric material.

To quantify the long-ranged ferroelectric interactions, in Fig. 4 we show the $\Lambda$ dependence of the coercive field $E_c$ for the central slices of the KNO and KTO layers (solid and open squares, respectively), determined from hysteresis loops such as those in Fig. 3. For the smallest modulation lengths, $E_c$ is the same for both the KNO and KTO layers and is very close to that of the KTN solid solution under the same strain conditions, denoted by a star in Fig. 4. For $\Lambda < 12$, $E_c$ for the KNO and KTO layers is identical and increases with increasing $\Lambda$ because the increased coupling within a single KNO layers more than compensates for the decrease in coupling between the KNO layers.[6] Also shown in Fig. 4 (solid circles) is the electric field required to switch an antiparallel arrangement of polarization in alternating KNO layers, a further measure of the interactions between KNO layers. We find that for $\Lambda < 12$, the antiparallel arrangement of polarizations in the KNO layers is completely unstable even in the absence of an applied electric field, a direct effect of the long-ranged ferroelectric interactions between KNO layers. Based on these results, we consider $\Lambda < 12$ to be the strong-coupling regime.

By contrast, for $\Lambda > 24$, the interactions between the now rather bulklike KNO layers is sufficiently weak that they respond essentially independently of each other; this is evidenced by $E_c$ for KNO increasing monotonically to its

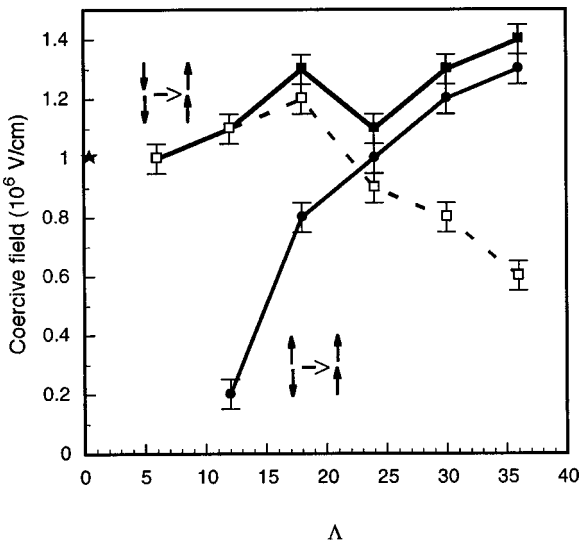


FIG. 4. Coercive fields $E_c$ in the interiors of the KNO and KTO layers as a function of modulation wavelength (solid and open squares), and the field required to switch an antiparallel arrangement of the polarizations of alternating KNO layers (solid circles), indicate the presence of regimes with strong ($\Lambda<12$) and weak ($\Lambda>24$) long-ranged ferroelectric interactions. The switching field for the KTN solid solution is indicated by the star.

asymptotic values of $2.5\times10^6$ V/cm, while $E_c$ for the KTO layer approaches zero. Moreover, $E_c$ for the switching of the antiparallel KNO layers tracks that of the switching of the superlattice. The relatively small difference in the $E_c$ in the two cases reflect the small residual interaction between the layers in this weak-coupling regime.

The behavior in the transition region, $12<\Lambda<24$, is more complicated. While the values of $E_c$ increase from $\Lambda=12$ to $\Lambda=18$, they are no longer identical for the KNO and KTO layers. Another aspect of the transition from strong to weak coupling is the decrease in $E_c$ over the range $18<\Lambda<24$ because the enhancement in $E_c$ as the KNO layers become thicker is not sufficient to compensate for the decrease in $E_c$ due to the decreasing interlayer coupling arising from the thicker KTO layers.

In summary, our simulations show that the effects of the interfaces and the effects of strain are largely decoupled in ferroelectric/paraelectric superlattices. We find that the long-ranged interactions between the ferroelectric layers are mediated by the induced dielectric response of the intervening paraelectric layers. This rather simple physics explains the observed strong modulation-length dependence of the properties of ferroelectric/paraelectric superlattices. Finally, the long-ranged ferroelectric interactions discussed here provide a conceptual framework in which to understand not only this particular ferroelectric/paraelectric superlattice but also the properties of other ferroelectric heterostructures.

We are happy to thank Stephen Streiffer, Orlando Auciello, David Norton, and Lynn Boatner for useful discussions. This work was supported by the U.S. Department of Energy, Office of Science, under Contract No. W-31-109-Eng-38 and by CONICET-Argentina.

[1] T. M. Shaw, A. Gupta, M. Y. Chern, P. E. Batson, R. B. Laibowitz, and B. A. Scott, J. Mater. Res. **9**, 2566 (1994).
[2] B. Q. Qu, M. Evstigneev, D. J. Johnson, and R. H. Prince, Appl. Phys. Lett. **72**, 1394 (1998).
[3] H. Tabata, H. Tanaka, and T. Kawai, Appl. Phys. Lett. **65**, 1970 (1994).
[4] H.-M. Christen, L. A. Boatner, J. D. Budai, M. F. Chisolm, L. A. Gea, P. J. Marrero, and D. P. Norton, Appl. Phys. Lett. **68**, 1488 (1996).
[5] H.-M. Christen, E. D. Specht, D. P. Norton, M. F. Chisolm, and L. A. Boatner, Appl. Phys. Lett. **72**, 2535 (1998).
[6] E. D. Specht, H.-M. Christen, D. P. Norton, and L. A. Boatner, Phys. Rev. Lett. **80**, 4317 (1998).
[7] J. C. Jiang, X. Q. Pan, W. Tian, C. D. Theis, and D. G. Schlom, Appl. Phys. Lett. **74**, 2851 (1999).
[8] F. L. Marrec, R. Farhi, M. E. Marssi, J. L. Dellis, M. G. Karkut, and D. Ariosa, Phys. Rev. B **61**, R6447 (2000).
[9] M. Sepliarsky, S. R. Phillpot, D. Wolf, M. G. Stachiotti, and R. L. Migoni, Appl. Phys. Lett. **76**, 3986 (2000).
[10] J. C. Slater, Phys. Rev. **78**, 748 (1950).
[11] M. D. Stiles, J. Magn. Magn. Mater. **200**, 322 (2000).